

## The Geometry of the Euclidean Hamiltonian Trajectories on $\sqrt[n]{1}$ Points

Blanca I. Niel

### Abstract

The Euclidean Hamiltonian Trajectory Problem may be expressed by means of an  $n$ -element vector  $\vec{p}$ , with  $p_i \in \{1, \dots, n\}$ . The points are originally presented as an ordered list of Cartesian coordinates at  $\mathbf{C}$  an  $n \times 2$  matrix, in which  $C_{j1}$  is the  $x$ -coordinate of the point  $j$ , and  $C_{j2}$  is the  $y$ -coordinate of the same point. We choose  $C_{j1} = \cos(\frac{2(j-1)\pi}{n})$ ,  $C_{j2} = \sin(\frac{2(j-1)\pi}{n})$  and  $j = 1, 2, \dots, n$ . We must also enforce  $p_i \neq p_j$ ,  $i, j \in \{1, \dots, n\}$   $i \neq j$  if all the points in the original list should belong to the final trajectory. The reordering may be achieved directly by means of an  $n \times n$  permutation matrix  $\mathbf{V}(\vec{p})$  defined by  $[\mathbf{V}(\vec{p})]_{ij} = 1$  if  $p_i = j$ , otherwise  $[\mathbf{V}(\vec{p})]_{ij} = 0$ . Consequently,  $\mathbf{V}(\vec{p}) \mathbf{C}$  contains the same point coordinates as  $\mathbf{C}$  but reordered in the manner defined by  $\vec{p}$ . Let  $\mathbf{D}$  be the  $n \times n$  matrix of negated interpoint distances given by  $D_{ij} = -(\text{euclidean distance between points } i \text{ and } j)$  and let  $\mathbf{Q}$  be the  $n \times n$  matrix given by  $Q_{ij} = \delta_{j-1,i} + \delta_{j+1,i}$   $i, j \in \{1, \dots, n\}$  here  $\delta_{ij}$  is the Kronecker tensor. Then the trajectory length corresponding to ordering  $\vec{p}$  is reached out in  $d(\vec{p}) = -\frac{1}{2} \text{trace}[\mathbf{V}(\vec{p}) \mathbf{D} \mathbf{V}(\vec{p})^T \mathbf{Q}]$ .

We pose four hamiltonian trajectory paradigms on a network built with  $\sqrt[n]{1}$  points as nodes, weighted by the euclidean distance amongst the nodes and an architecture of a complete graph  $K_n$  :

i)

$$\min_{\vec{p}} d(\vec{p})$$

ii)

$$\min_{\vec{p}} \frac{1}{2} \sum_{i=1}^n \sum_l \min_k \sum_{k \neq l} D_{l,k} V_{l,i} (V_{k,i+1}(\vec{p}) + V_{k,i-1}(\vec{p}))$$

iii)

$$\max_{\vec{p}} d(\vec{p})$$

iv)

$$\max_{\vec{p}} \frac{1}{2} \sum_{i=1}^n \sum_l \max_k \sum_{k \neq l} D_{l,k} V_{l,i} (V_{k,i+1}(\vec{p}) + V_{k,i-1}(\vec{p}))$$

We overcome these paradigms looking at the inherent geometrical core of the particular set of points that we deal with. Our contribution provide entire answers that could be utilized to validate the approximation techniques implemented in order to render suboptimal solutions of these benchmark problems.

Namely, is easy to demonstrate that the minimum strategy criteria have the same responses. Precisely, the regular configurational shape that realize the optimal are the piecemeal lines conforming the perimeter of the  $n$ -polygons on the  $\sqrt[n]{1}$  points. Another easy task is to find the minimum and maximum bounds for the problems. Worthy to notice is that maximum strategy criteria go aside when even or odd number of nodes are considered. At the odd node instances these strategies are baited for the lure of the perfect shape, since the optimal configurations are attained by the piecemeal lines of the odd  $n$ -star polygons of maximum density. While even nodes cases the optimal configuration shapes look less regular. By the way, there are structural differences between the representative configurations of each distinct valuated even-maximum strategies.

## 1 Introduction

We fairly solve an Euclidean Hamiltonian Cycle Problem on the  $n$  points of the  $n^{\text{th}}$  roots of 1, these  $n$  points represent the roots of the cyclotomic equation  $z^n = 1$   $n \in \mathbb{N} \cup \{0\}$  and straightforward computed by the Moivre's Theorem. We obtain the vertices of a regular  $n$ -polygon, inscribed in the circle  $|z| = 1$ . The architecture of the network, after the number of nodes  $n$  has been established, conforms a complete graph  $K_n$ , i.e., its whole linkage between nodes has  $\binom{n}{2}$  connections and it is regular of degree  $n - 1$ . The internode weights of the network is the euclidean distance between the  $n$  points of the  $n^{\text{th}}$ -roots of 1. We querying about the hamiltonian cyclic configurations which reach out the minimum global, the maximum global, the nearest neighbor sequential minimum (greediest step by step strategy) and the farthest neighbor sequential maximum (clumsiest step by step strategy) on the complete strongly connected  $K_n$  directed graph architecture of the symmetrical euclidean weighted network. We must then find a optimum-weight hamiltonian cycle in the resultant network. This problem is certainly  $\mathcal{NP}$ -complete [1], because if all the edge weights are made to equal one, the problem reduces to the  $\mathcal{NP}$ -complete problem of finds out all the hamiltonian cycles in a  $K_n$  graph. Sometimes the overridden concern is minimizing total cost or travel time rather than distance. In an euclidean distance weighted and strongly connected graph there exist nodes  $s$  and  $t$  on distinct graph geodesics passing through  $u$  and  $v$  nodes where the triangle inequality  $d(s, t) \leq d(s, v) + d(v, t)$  holds on. In the brachistochrone instances, the triangle inequality rarely holds on. Our euclidean hamiltonian global optimum criteria involve tougher theoretical and computational tasks since the network with its  $K_n$  graph architecture has  $\frac{(n-1)!}{2}$  hamiltonian cycles [2]. Even for moderate number of nodes  $n$ , checking all such cycles would be ludicrous as we had experienced in simulations <sup>1</sup> performed in 1998 [3].

<sup>1</sup>Processing Times with a Pentium 133 Mhz, 32 R.A.M. Mbytes, Linux Operative System, and C++ software programming language

- 1) 10 nodes, 2 seconds.
- 2) 11 nodes, 15 seconds.
- 3) 13 nodes, 5.38 minutes.

Thus other approaches are called for, known as approximation techniques. A common approximation methods use a local greedy algorithmic approach. This method produces early savings in edge weights, but could be far from optimal when the cycle is formed. An outcome of the greedy and clumsy techniques (which are known as the nearest and farthest neighbor method) requires beforehand the knowledge of the lower and upper bounds of the problem in order to conclude if the suboptimal found is reasonably close to the true optimal. Consequently, we find both required bounds. Then we set apart the trivial networks with three and four nodes, and subsequently we tidily resolve the paradigms for any arbitrary number of nodes.

In this paper, we use the geometric structure inherent of the  $n$  points of the  $n^{\text{th}}$ -roots of 1 to shed a new light on the relationship between euclidean geometry of polygons, digons and stargons and four distinct strategies involving the search of euclidean hamiltonian cyclic trajectories on the  $n$  points of the  $\sqrt[n]{1}$ . Firstly, we explain the theoretical context of the problem. Secondly, in Section 2 we introduce the notation relevant to the rest of the paper and we formulate mathematically the subject of our concern. In Section 3 we review the mathematics background of  $n$ -regular polygons and  $n$ -star regular polygons, all geometric shapes that should be distinguishable in terms of if the number of vertices are even, odd primes and odd not primes. In Section 4 we describe the architecture of the network in the context of graph theory. We also identify the circulant graphs as those that will be adequate to show the active nodes for some optimal configurations. In Section 5 we expose the core of our results. In Section 6 we detail collateral derivations to the central material of this research in order to bring about an application from the perspective of light ray propagation time on the quasi-spherical mirrors as well as some ancillary information of the reflection law behavior at the spherical mirror. Finally, we presents the general conclusions.

## 2 Euclidean Hamiltonian Trajectory Problem Formulation

The Euclidean Hamiltonian Trajectory Problem may be expressed by means of an  $n$ -element vector  $\vec{p}$ , with  $p_i \in \{1, \dots, n\}$ . The points are originally presented as an ordered list of Cartesian coordinates at  $\mathbf{C}$  an  $n \times 2$  matrix, in which  $C_{j1}$  is the  $x$ - coordinate of the point  $j$ , and  $C_{j2}$  is the  $y$ - coordinate of the same point. We choose

$$C_{j1} = \cos\left(\frac{2(j-1)\pi}{n}\right), \quad C_{j2} = \sin\left(\frac{2(j-1)\pi}{n}\right) \quad \text{and} \quad j = 1, 2, \dots, n. \quad (1)$$

We must also enforce

$$p_i \neq p_j, \quad i, j \in \{1, \dots, n\} \quad i \neq j$$

if all the points in the original list should belong to the final trajectory. The reordering may be achieved directly by means of an  $n \times n$  permutation matrix  $\mathbf{V}(\vec{p})$  [4, 5] defined

- 
- 4) 13 nodes, 69.68 minutes.
  - 5) 14 nodes, 971.32 minutes.
  - 6) 15 nodes, 9266 minutes, 6.43 days.
  - 7) 60 nodes, the required processing time would be  $10^{52}$  millions of years.

by

$$[\mathbf{V}(\vec{\mathbf{p}})]_{ij} = \begin{cases} 1, & \text{if } p_i = j \\ 0, & \text{otherwise.} \end{cases} \quad (2)$$

Consequently,

$$\mathbf{C}' = \mathbf{V}(\vec{\mathbf{p}}) \mathbf{C}$$

$\mathbf{C}'$  contains the same point coordinates as  $\mathbf{C}$  but reordered in the manner defined by  $\vec{\mathbf{p}}$ . The components of  $\mathbf{V}(\vec{\mathbf{p}})$  are all ones or zeros, an each row and column contains only a single one. Expressed mathematically and neatly

$$\mathbf{V}(\vec{\mathbf{p}}) = \mathbf{R}^n \mathbf{V}(\vec{\mathbf{p}}) \mathbf{R}^n + \mathbf{S}$$

here

$$\mathbf{R}^n = \mathbf{I}^n - \frac{\mathbf{O}^n}{n}$$

$$\mathbf{S} = \frac{\mathbf{O}^n}{n}$$

with  $\mathbf{I}^n$  be the  $n \times n$  identity matrix and  $\mathbf{O}^n$  be the  $n \times n$  matrix of ones. Let  $\mathbf{D}$  be the  $n \times n$  matrix of negated interpoint distances given by

$$D_{ij} = -(\text{euclidean distance between points } i \text{ and } j)$$

and let  $\mathbf{Q}$  be the  $n \times n$  matrix given by

$$Q_{ij} = \delta_{j-1,i} + \delta_{j+1,i} \quad i, j \in \{1, \dots, n\}$$

here  $\delta_{ij}$  is the Kronecker tensor [6]

$$\delta_{ij} = \begin{cases} 1, & \text{if } i = j \\ 0, & \text{if } i \neq j. \end{cases}$$

Then the trajectory length corresponding to ordering  $\mathbf{p}$  is reached out in

$$d(\vec{\mathbf{p}}) = -\frac{1}{2} \text{trace}[\mathbf{V}(\vec{\mathbf{p}}) \mathbf{D} \mathbf{V}(\vec{\mathbf{p}})^\top \mathbf{Q}]. \quad (3)$$

We pose four hamiltonian trajectory paradigms on a network [7, 8] built with  $\sqrt[3]{1}$  points as nodes, weighted by the euclidean distance amongst the nodes and an architecture of a complete graph  $K_n$  :

i)

$$\min_{\mathbf{p}} d(\vec{\mathbf{p}}) \quad (4)$$

ii)

$$\min_{\vec{\mathbf{p}}} \frac{1}{2} \sum_{i=1}^n \sum_l \min_k \sum_{k \neq l} D_{l,k} V_{l,i} (V_{k,i+1}(\vec{\mathbf{p}}) + V_{k,i-1}(\vec{\mathbf{p}})) \quad (5)$$

At the previous equation we were assuming that  $\vec{\mathbf{p}}$  are hamiltonian cycle trajectories. The above equation is the Lyapunov function associated to the network is built by adding up the followings terms for every pair of distinct points  $l, k$  whenever both

points are adjacent in a candidate cycle, i.e., when  $V_{l,i} = 1$  and  $V_{k,i\pm 1} = 1$  for any  $i$ . Since each node output value is either 0 or 1, we obtain

$$\sum_{i=1}^n D_{l,k} V_{l,i} (V_{k,i+1} + V_{k,i-1})$$

The factor  $\frac{1}{2}$  chops the ambiguity from direct and opposite cycle reckoning.

iii)

$$\max_{\mathbf{p}} d(\vec{\mathbf{p}}) \quad (6)$$

iv)

$$\max_{\vec{\mathbf{p}}} \frac{1}{2} \sum_{i=1}^n \sum_l \max_k \sum_{k \neq l} D_{l,k} V_{l,i} (V_{k,i+1}(\vec{\mathbf{p}}) + V_{k,i-1}(\vec{\mathbf{p}})) \quad (7)$$

The equations (5) and (7) had been built with the entries of  $\mathbf{V}(\vec{\mathbf{p}})^T$  [9, 10, 11]. We employ *periodic boundary conditions*, so that the top and bottom elements in a column are regarded as neighbors, as are the leftmost and rightmost elements in a row. We choose boolean binary nodes  $V_{l,i}$  to represent if and only if the point  $l$  is the  $i^{\text{th}}$  stop on the cycle. There are  $n^2$  node outputs in all. Note that there are  $2n$  equivalent formal solutions for each optimal cycle, since we do not care where we start the cycle or which direction we go around it. However, the network represents these possibilities by different configurations. One point can be clamped (e.g., so city 1 is always at stop 1) if it is desired to break this degeneracy.

## 3 Geometry

### 3.1 Regular Polygons

Rotations about a fixed point  $O$  through angles  $\theta, 2\theta, 3\theta, \dots$  transform any point  $P_0$  (distinct from  $O$ ) into other points  $P_1, P_2, P_3, \dots$  on the circle with center  $O$  and radius  $OP_0$ . In general these points become increasingly dense on the circle; but if the  $\theta$  is commensurable with a right angle, only a finite number of them will be distinct. In particular, if  $\theta = \frac{2\pi}{n}$ , where  $n$  is a positive integer greater than 2, then there will be  $n$  points  $P_k$  whose successive joins  $P_0P_1, P_1P_2, \dots, P_{n-1}P_0$  are the sides of an ordinary regular  $n$ -polygon.

For brevity's sake we assume  $OP_0 = 1$ ,  $P_0 = (1, 0)$  and the  $P_k$  points are obtained by the Moivre's Formula applied to solve the equation for  $z \in \mathbb{C}$

$$z^n = 1$$

$$\sqrt[n]{\omega} = \sqrt[n]{|\omega|} \left( \cos\left(\frac{\text{Arg}\omega + 2k\pi}{n}\right) + i \sin\left(\frac{\text{Arg}\omega + 2k\pi}{n}\right) \right) \quad k = 0, 1, \dots, n-1.$$

The previous considerations let it be

$$\sqrt[n]{1} = \sqrt[n]{|1|} \left( \cos\left(\frac{0 + 2k\pi}{n}\right) + i \sin\left(\frac{0 + 2k\pi}{n}\right) \right) \quad k = 0, 1, \dots, n-1. \quad (8)$$

### 3.2 Star Polygons

Let us now extend this notion by allowing  $n$  to be any rational number greater than 2, say the fraction  $\frac{p}{d}$  (where  $p$  and  $d$  are coprime). Accordingly, we define a (generalized) regular polygon  $\{n\}$ , where  $n = \frac{p}{d}$ . Its  $p$  vertices are derived from  $P_0$  by repeated rotations through  $\frac{2\pi}{n}$ , and its  $p$  sides (enclosing the center  $d$  times) are

$$P_0P_1, P_1P_2, \dots, P_{p-1}P_0.$$

Since a ray coming out from the center without passing through a vertex will cross  $d$  of the  $p$  sides, this denominator  $d$  is called the *density* of the polygon. When  $d = 1$ , so that  $n = p$ , we have the ordinary regular  $p$ -polygon  $\{p\}$ . When  $d \geq 1$ , the sides cross one another, but the crossing points are not counted as vertices. Since  $d$  may be any positive integer relatively prime to  $p$  and less than  $\frac{p}{2}$ , there is a regular polygon  $\{n\}$  for each rational number  $n \geq 2$ . In fact, it is occasionally desired to include also the *digon*  $\{2\}$ , although its two sides coincide. When  $p = 5$ , we have the pentagon  $\{5\}$  of density 1 and the *pentagram*  $\{\frac{5}{2}\}$ , which was the Pythagorean symbol of good health.

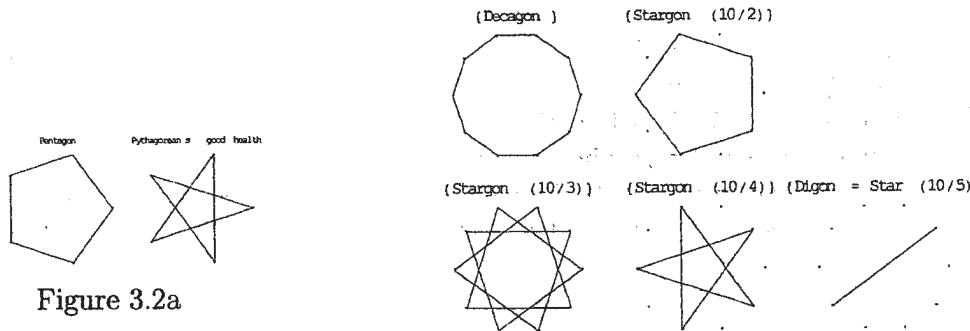


Figure 3.2a

Figure 3.2b

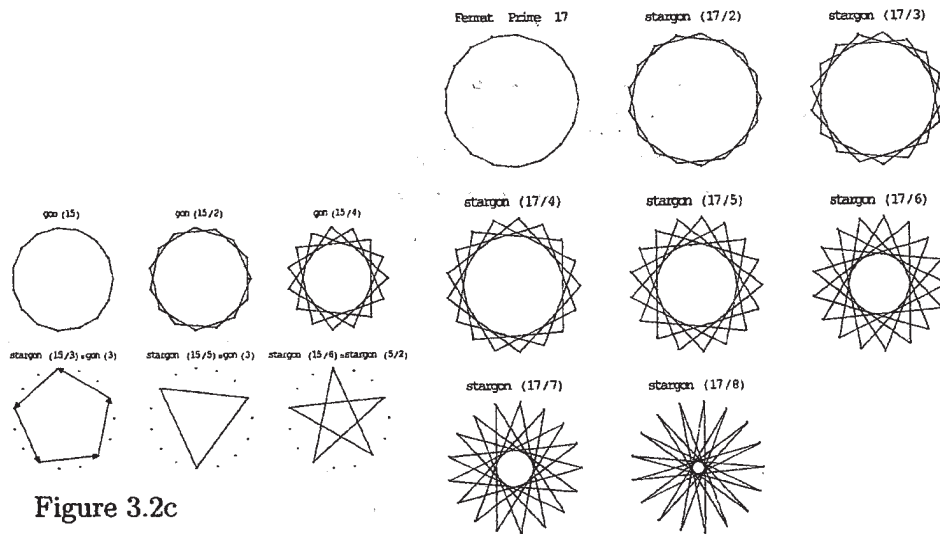


Figure 3.2c

Figure 3.2d

Figure 3.2c shows all of the stargons corresponding to the *odd number 15* and Figure 3.2d sketch all of the regular star polygons of the *Fermat's prime number 17*. Polygon for *Actas del VI Congreso Dr. A. A. R. Monteiro, 2001*

which  $d > 1$  are known as *star polygons* [12].

Let  $D_n$  be the symmetry group of the regular  $n$ -polygon,  $\{n\}$ , this group of order  $2n$  consists of  $n$  rotations and  $n$  reflections through the  $n$  effectively distinct multiples of  $\frac{2\pi}{n}$ . A practical way to make a model of  $D_n$  is to join two ordinary mirrors by a hinge and stand them on the lines  $OP_i$  and  $OP_{M_{P_i P_{i\pm 1}}}$  with  $P_i$  and  $P_{i\pm 1}$  a vertex and its next or foregoing midpoint on a regular  $n$ -gon, respectively. Therefore both mirrors are inclined at  $\frac{\pi}{n}$ .

### 3.2.1 $n$ - odd Geometry

From the general dihedral group  $D_n$ , when  $n$  is odd, each of the  $n$  mirrors ( $n$  reflections,  $n$  rotations of  $\frac{2\pi}{n}$  multiples) joins a vertex of an  $n$ -regular polygon to the midpoint of the opposite side.

### 3.2.2 $n$ - even Geometry

From the general dihedral group  $D_n$ , when  $n$  is even,  $\frac{n}{2}$  mirrors join pairs of opposite vertices and  $\frac{n}{2}$  bisect pairs of opposite sides.

## 3.3 The Principle of Least Time

The following are the important facts of ray optics well known in Fermat's lifetime [13]:

- i) light travels in straight lines in uniform media,
- ii) light reflects from mirror like a billiard ball bouncing from a pool table bumper (Figure 3.3a),
- iii) when passing from a less dense material (e.g., air) into a more dense material (e.g., water) light rays incline (i.e., refract) toward the interface normal (Figure 3.3b), and
- iv) light ray are reversible, that is, light can propagate in either direction along the same path.

According to Fermat's Principle of Least Time, light propagates between two points in such a way as to minimize its travel time (brachistochrones). Descarte's followers were quick to point out a difficulty with the Principle of Least Time, because the light reflection law is sometimes consistent with the greatest rather than the least propagation time (e.g., spherical mirror).

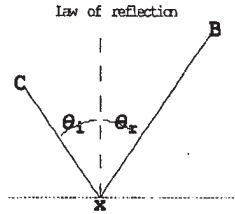


Figure 3.3a

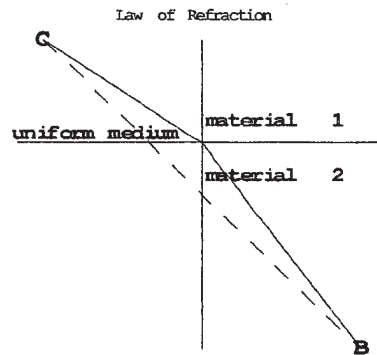


Figure 3.3b

## 4 Network Architecture

### 4.1 Circulant Graphs

The networks have the architecture of *complete graphs*  $K_n$ , with  $\binom{n}{2}$  (i.e.,  $\frac{n(n-1)}{2}$ ) edges and are regular of degree  $n - 1$ , because feedbacks are not allowed. Inside these maximum connectivity graphs we sift out the *circulant graphs* and more properly *circulant digraphs* [14] since its play an important role in the connections of optimal trajectories. Let  $n_1, n_2, \dots, n_k$  be a sequence on positive integers where  $0 < n_1 < n_2 < \dots < n_k < \frac{(n+1)}{2}$ . Then the *circulant graph*  $\tilde{C}_n(n_1, n_2, \dots, n_k)$  is the graph on  $n$  nodes  $v_1, v_2, \dots, v_n$  with vertex  $v_i$  adjacent to each vertex  $v_{i \pm n_j \pmod{n}}$ . The values  $n_i$  are called *jump sizes*. Now the corresponding *directed circulant* is defined similarly, except that adjacent with is replaced by adjacent to.

## 5 Euclidean Hamiltonian Trajectory Resolution

### 5.1 Two particularly simple cases $n = 3$ , $n = 4$

The simplest case,  $K_3$  is the equilateral triangle (Figure 5.1a). Its inherent geometry does not shed new light on the general instances. A unique answer to the distinct strategies  $D_{\min} = D_{+\epsilon} = D_{\max} = D_{-\epsilon} = 3\sqrt{3} \approx 5.19615$ .

The set of points  $\sqrt[4]{1}$  with associated  $K_4$ 's architecture network and synaptic tensor given by the euclidean distances amongst the nodes bring about a twilight over the complete landscape of the generalized weighted network of our aim. This special case only distinguishes network's performance between minimum and maximum criteria (Figure 5.1b). Greediest strategy and global minimum are the same  $D_{\min} = D_{+\epsilon} = 4 * \sqrt{2}$ . On the contrary, clumsiest strategy and global maximum are the same  $D_{\max} = D_{-\epsilon} = 2*2+2*\sqrt{2}$ .



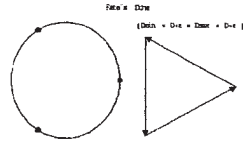


Figure 5.1a

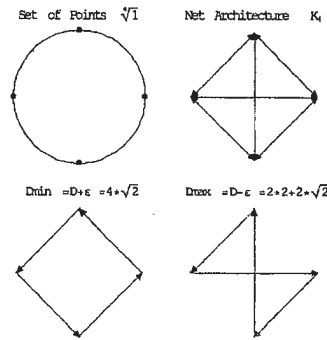


Figure 5.1b

Nevertheless, these special instances do not bring about the understanding of our goal.

### 5.2 Hamiltonian Path Problem Bounds

The upper and lower bounds for the euclidean hamiltonian cycle problem are easily obtained, let  $C_H$  be any arbitrary hamiltonian cycle configuration  $\vec{p}$ , so

$$2\pi \leq \sum_{(k,l) \in C_H} \text{chord length}_{kl} = \sum_{(k,l) \in C_H} D_{k,l} \leq 2n \tag{9}$$

### 5.3 Both Minimum Criteria

At the first glance, the same answer to both minimum criteria is easily recognizable. By geometrical considerations or by taking a look inside the distance matrices  $D$ , which have structured matrices as the shown pattern below  $D_{\min} = D_{l,l+1}$

$$\begin{pmatrix} 0 & D_{l,l+1} & * & * & \dots & D_{l,l+1} \\ D_{l,l+1} & 0 & D_{l,l+1} & * & \dots & * \\ & D_{l,l+1} & 0 & D_{l,l+1} & * & * \\ & * & D_{l,l+1} & 0 & D_{l,l+1} & * \\ \dots & \dots & \dots & \dots & \dots & \dots \\ D_{l,l+1} & * & * & * & D_{l,l+1} & 0 \end{pmatrix}$$

since  $D_{k,l} \geq D_{l,l+1} = \min D_{k,l} = D_{\min} = \sqrt{2} \sqrt{1 - \cos \frac{2\pi}{n}}$  and  $*$  labels entries with  $*$  =  $D_{k,l} > D_{l,l+1}$ . Consequently, the optimal configuration is  $\vec{p} = \{1, 2, \dots, n, 1\}$  and its reverse  $\vec{p} = \{1, n, \dots, 2, 1\}$

The search is “greedy ”[1] because at every step it chooses the shortest distance it can, without worrying whether this will prove to be sound decision in the long run. Furthermore it never changes its mind: once a point has been included in the solution, it is there for good. This approach produces early savings in edge weights, but could be far optimal when the cycle is formed. In the instance of our concern the geometrical distribution of the points falls apart the right prejudice about the greedy methods. Here greedy optimum is the optimal, i.e. paradigms *i*) and *ii*) have the same responses.

$$\begin{aligned}
\min_{\vec{p}} d(\vec{p}) &= \text{Equation(5)} = \min_{\vec{p}} \frac{1}{2} \sum_{i=1}^n \sum_l D_{l,l+1} V_{l,i} (V_{l+1,i+1}(\vec{p}) + V_{l+1,i-1}(\vec{p})) = \\
&= \sum_{l=1}^n D_{l,l+1} V_{l,l} (V_{l+1,l+1}(\vec{p}) + V_{l+1,l-1}(\vec{p})) = \sum_{l=1}^n D_{l,l+1} = n D_{12} = \\
d_{\text{greedy}} &= d_{\text{minimum}} = n \sqrt{2} \sqrt{1 - \cos \frac{2\pi}{n}} \quad (10)
\end{aligned}$$

with  $\vec{p} = \{1, 2, \dots, n\}$  and its reverse  $\vec{p} = \{n, n-1, \dots, 1\}$  as the configurations which realized optima for both minimum criteria. Since any other choices involve to go off the optima. For each one of the previous direct and opposite configurations there are  $n$  equivalent formal solutions corresponding to the possibility of  $n$  distinct choices as departure point.

#### 5.4 Both Maximum Criteria

i) Odd number of nodes  $n = 2k + 1$ ,  $k \geq 2$ , here clumsy strategy is the optimal, that is

$$\max_{\vec{p}} d(\vec{p}) = \max_{\vec{p}} \frac{1}{2} \sum_{i=1}^n \sum_l \max_k \sum_{k \neq l} D_{l,k} V_{l,i} (V_{k,i+1}(\vec{p}) + V_{k,i-1}(\vec{p}))$$

$$\begin{aligned}
D_{k,l} &\leq D_{\max} = D_{l, \lfloor \frac{2k+1}{2} \rfloor + l} \\
D_{k,l} &= *_{k,l} < D_{\max}
\end{aligned}$$

$$\left( \begin{array}{cccccccccc}
0 & * & * & * & D_{\max} & D_{\max} & * & * & * \\
* & 0 & * & * & * & D_{\max} & D_{\max} & * & * \\
* & * & 0 & * & * & * & D_{\max} & D_{\max} & * \\
* & * & * & 0 & * & * & * & D_{\max} & D_{\max} \\
D_{\max} & * & * & * & 0 & * & * & * & D_{\max} \\
D_{\max} & D_{\max} & * & * & * & 0 & * & * & * \\
* & D_{\max} & D_{\max} & * & * & * & 0 & * & * \\
* & * & D_{\max} & D_{\max} & * & * & * & 0 & * \\
* & * & * & D_{\max} & D_{\max} & * & * & * & 0
\end{array} \right)$$

If  $n$  is odd, so  $n = 2k + 1$   $k \geq 5$  the cardinality ( $\#$ ) of the set  $\{D_{k,l} \neq D_{\max}\}$  in each row is  $\#\{D_{k,l} \neq D_{\max}\} = n - 2$ , and structures of subsequent rows are cyclotomic after one arbitrary node had been labeled as the first. From it to the node places at the configurational position  $\lfloor \frac{2k+1}{2} \rfloor$  and  $\lfloor \frac{2k+1}{2} \rfloor + 1$  should be allocated consecutively both  $D_{\max}$

$$D_{\max} = D_{l, l + \lfloor \frac{2k+1}{2} \rfloor} = D_{1, 1 + \lfloor \frac{2k+1}{2} \rfloor} = \sqrt{2} \sqrt{1 - \cos \frac{2 \lfloor \frac{2k+1}{2} \rfloor \pi}{2k+1}}$$

$$\max_{\vec{p}} d(\vec{p}) = \frac{1}{2} \sum_{i=1}^n \sum_l D_{l, l + \lfloor \frac{2k+1}{2} \rfloor} V_{l,i} (V_{l + \lfloor \frac{2k+1}{2} \rfloor, i+1}(\vec{p}) + V_{l + \lfloor \frac{2k+1}{2} \rfloor, i-1}(\vec{p}))$$

The previous equations run properly under the constraints of periodic boundary conditions. For brevity's sake we clamped the initial point at  $l$  and tracked down the paths from  $l$  in the increasing order of the configurational stop.

$$\sum_l D_{l, l + \lfloor \frac{2k+1}{2} \rfloor} = n\sqrt{2} \sqrt{1 - \cos \frac{2 \lfloor \frac{2k+1}{2} \rfloor \pi}{2k+1}} \quad (11)$$

Here  $\vec{p}$  are the  $2n$  equivalent formal solutions for each optimal cycle, since we do not care where we start the cycle or which direction we go around it. However, the network represents these possibilities by different configurations. One city can be clamped (e.g., so city 1 is always at stop 1) to break this degeneracy if desired.

- ii) Even number of nodes  $n = 2k$   $k \geq 3$   $D_{\max} = 2$  there is only one  $D_{\max}$  on each line. The geometrical meaning of it is the existence of all diametric opposite points between each other, when the  $2k$  of the  $2k^{\text{th}}$  points of  $\sqrt[2k]{1}$  are considered. The matrix below shows the sites allocated by the farthest neighbor, the almost farthest neighbor and the nearest neighbor, the  $D_{\max} = 2$ ,  $D_{aw} = \sqrt{2(1 - \cos(\pi - \frac{\pi}{k}))}$  the distance between the almost farthest neighbor and the nearest neighbor  $D_{\min} = D_{l, l+1} = \sqrt{2(1 - \cos \frac{\pi}{k})}$  all these expression must be evaluated taking into account that  $n = 2k$  with  $k \geq 3$ .

$$\begin{pmatrix} 0 & D_{l, l+1} & * & * & D_{aw} & 2 & D_{aw} & * & * & D_{l, l+1} \\ D_{l, l+1} & 0 & D_{l, l+1} & * & * & D_{aw} & 2 & D_{aw} & * & * \\ * & D_{l, l+1} & 0 & D_{l, l+1} & * & * & D_{aw} & 2 & D_{aw} & * \\ * & * & D_{l, l+1} & 0 & D_{l, l+1} & * & * & D_{aw} & 2 & D_{aw} \\ D_{aw} & * & * & D_{l, l+1} & 0 & D_{l, l+1} & * & * & D_{aw} & 2 \\ 2 & D_{aw} & * & * & D_{l, l+1} & 0 & D_{l, l+1} & * & * & D_{aw} \\ D_{aw} & 2 & D_{aw} & * & * & D_{l, l+1} & 0 & D_{l, l+1} & * & * \\ * & D_{aw} & 2 & D_{aw} & * & * & D_{l, l+1} & 0 & D_{l, l+1} & * \\ * & * & D_{aw} & 2 & D_{aw} & * & * & D_{l, l+1} & 0 & D_{l, l+1} \\ D_{l, l+1} & * & * & D_{aw} & 2 & D_{aw} & * & * & D_{l, l+1} & 0 \end{pmatrix}$$

**Clumsiest.** The reversal strategy to be the greediest. After the initial point had been chosen, the reversal greedy strategy, from now on forwards named as the clumsiest -step by step- search run straightforward from the initial chosen point to its diametric opposite point. Even though the method is engaged to make step by step the worst chosen amongst all none picked out points, after the cycle was formed the clumsy technique was far from the worst in our instance.

For the sake of argument suppose the point  $(1, 0)$  is selected as the initial the clumsy strategy go straight to its diametrical opposite point it has not the worst choice since the cycle is closed in the  $n$ -digon shape (it is neatly not a hamiltonian cycle).

$$\begin{aligned} & \max_{\vec{p}} \frac{1}{2} \sum_{i=1}^n \sum_l \max_k \sum_{k \neq l} D_{l, k} V_{l, i} (V_{k, i+1}(\vec{p}) + V_{k, i-1}(\vec{p})) = \\ & = \max_{\vec{p}} \frac{1}{2} \left\{ \sum_{i=1}^n \sum_{l=1}^k (D_{l, l+\frac{2k}{2}} + D_{l+\frac{2k}{2}, l+1}) V_{l, i} (V_{l+\frac{2k}{2}, i+1}(\vec{p}) + V_{l+\frac{2k}{2}, i-1}(\vec{p})) \right\} + D_{l, l+1} \end{aligned}$$

Consequently, clumsy strategy at the second stage chooses the worst amongst the possible not picked out points, which implicated any of the nearest neighbor of its diametrically located point  $D_{aw} = D_{nndo} = \sqrt{2}\sqrt{1 - \cos \frac{2\pi(k-1)}{2k}}$   $k \geq 3$ , concisely  $D_{aw} = \sqrt{2}\sqrt{1 - \cos(\pi - \frac{\pi}{k})}$   $k \geq 3$ , once the third selection is done, once more the latest point included in the cycle has the possibility to reach out its antipodal, and over and over this occur until the  $n - 1$  stage in which no choice is allowed because is needed to turn back. A slightly calculation allow us recognize that if there are  $2k$ ,  $k \geq 3$  piecemeal lines  $\frac{2k}{2}$  pass through diametrical opposite ends, other  $\frac{2k}{2} - 1$  go through the nearest neighbor of its diametrical opposite and only one, the latest pace, between nearest neighbors. Therefore the total track maximum distance is with  $k \geq 3$

$$d_{\text{clumsy}} = k * 2 + (2k - (k + 1)) * \sqrt{2}\sqrt{1 - \cos(\pi - \frac{\pi}{k})} + \sqrt{2}\sqrt{1 - \cos(\frac{\pi}{k})} \quad (12)$$

Even though the clumsy strategy is engaged to be the worst, it can not reach out its commitment in our instance. This search struggles so harsh at the early stages making the worse decision as possible than the more compensatory unfavorable search that properly realized the maximum.

**Worst.** The reversal strategy to be the best. The worst or farthest trajectory begets a balance between the antipodal node choices and the nearest antipodal node choices. Here the farthest walk is realized by configurations of hamiltonian cycles conform with two antipodal tracks (step length 2), and  $2k - 2$  almost antipodal tracks (step length  $\sqrt{2}\sqrt{1 - \cos(\pi - \frac{\pi}{k})}$ ). Therefore the total track maximum distance is  $d_{\text{max}} = 2 * 2 + (2k - 2) * \sqrt{2}\sqrt{1 - \cos(\pi - \frac{\pi}{k})}$  with  $k \geq 3$ .

$$\max_{\vec{p}} d(\vec{p}) = 2 * 2 + (2k - 2) * \sqrt{2}\sqrt{1 - \cos(\pi - \frac{\pi}{k})} \quad (13)$$

## 5.5 The Representative Euclidean Hamiltonian Cycles

We pointed out that there are more than one formal solution for each optimal cycle. The next figure (Figure 5.1.1 a, Figure 5.1.1 b) shows some representative trajectories of the optimal cycles for the sake of fostering comparison between even and odd network's order instances. On the sketch the optimal trajectories are placed together inside the left ( $n = 10$ ) and right ( $n = 17$ ) frame, respectively.

### 5.5.1 The point positions on the traveled path with distinct optimal hamiltonian cycles

Figure 5.5.1a shows from left to right the standard pattern of the shortest (minimum  $\equiv$  greediest) hamiltonian cycles, a path corresponding to the farthest ( $\equiv$  maximum) cycles and the clumsiest strategy ( $\equiv$  anti-greediest) cycles for even number of nodes, particularly  $n = 10$ . The left and the right trajectories inside this frame should be considered as a representative module the symmetry group of its respective figure. It means module their symmetry operations they beget optimal uniqueness. In contrast, the central path could not be considered as a the unique representative module its symmetry operations.

A glance over Figure 5.5.1b addresses us to the conclusion that both optimal trajectories

(minimum  $\equiv$  greediest, maximum  $\equiv$  clumsiest) module rotations and translations beget optimal uniqueness.

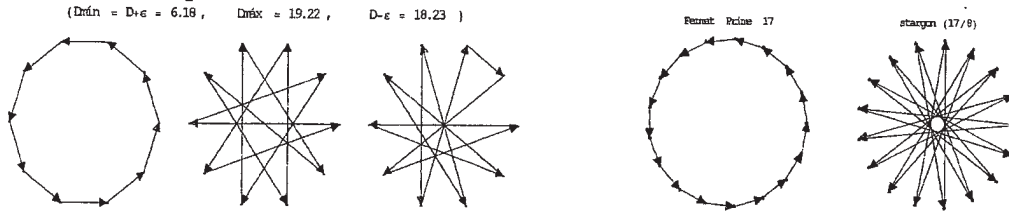


Figure 5.5.1a

Figure 5.5.1b

### 5.5.2 Network Node's Activities on the Optimal Trajectories

The activity of each boolean node in the network on the optimal trajectories are portrayed by the circulant digraphs. Minimum active connectivities are depicted by  $\tilde{C}(n, 1)$ , and odd-network maximum active connectivities are sketched by  $\tilde{C}(n, \lfloor \frac{n}{2} \rfloor)$ . In contrast, circulant digraphs are unable to represent the optima when the network is conformed by an even number of points, since the absence of regularity at the optima trajectories. Figure 5.5.2 from left to right shows a representative for the minimum ( $\equiv$  greediest), a representative for the path of the maximum star regular polygon (neither maximum nor minimum), a representative cycle for the anti-greedy strategy (clumsiest) and one of the possible representation for the maximum strategy. The absence of regularity on the optimal paths make failure the possibility of the use of circulant digraphs in order to display the network node's activities at any attainable even-maximum.

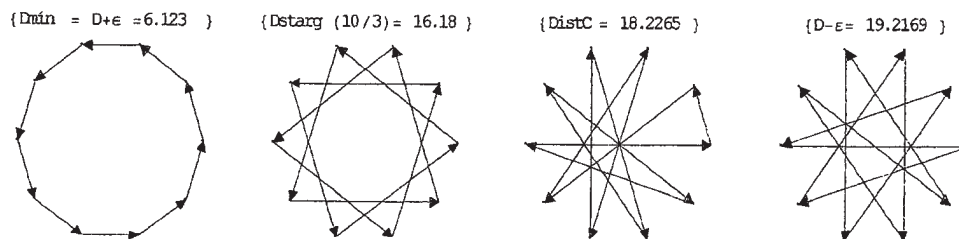


Figure 5.5.2

## 6 Epilogistic Application

Focusing on the *Principle of Least Time* (Section 3.3), our contribution makes evident that rays obeying *the law of reflection*<sup>2</sup> occasionally maximize or minimize ray travel time and there are even valid ray paths which neither maximize nor minimize the travel time function. Previously to the explanation of this breakthrough at the quasi-spherical mirrors let us compare, the reflection law on some light paths over the spherical mirror (Figure 6). We choose two different ray paths both of which start at the center  $C$  of a spherical mirror of radius  $CA$ , reflect once, and return to a point  $B$  on the axis behind the center after reflection. One ray reflects at  $A$  and the other at  $D$ . The ray path  $CDB$  which approaches the mirror head-on and returns along a diameter is the only one con-

<sup>2</sup>Hero's Problem, 125 B.C., Alexandria (Figure 3.3a).

sistent with the reflection rule ( $\theta_i = \theta_r$ ). It is also longer than neighboring paths such as CAB ( $\theta_i \neq \theta_r$ ) and for this reason has a longer propagation time. Light sometimes follows the longer path (CDB) between two points (C and B). An analytical proof that the ray CDB maximizes the propagation time, comes out from the geometry of a *Spherical Mirror*. Let  $R = CA = AE$  and  $\alpha = \angle DCA$ . The propagation time function  $T(\alpha)$  is maximized for  $\alpha = 0$  and minimized for  $\alpha = \pi$ . Let  $l(\alpha)$  be the total length traveled by a possible light ray that follow the track sketched on the Figure 6 called CAB. The endpoints of the trajectories are placed inside a uniform medium, consequently the ray lights travel straightfoward, i.e., on straight lines. By the way, the task of looking for stationary points of the light propagation time function  $T(\alpha)$  is equivalent to search for critic points of the total length traveled by a possible light ray module the light velocity constant  $c \approx 300000 \frac{km}{seg}$  of the specific medium, consequently  $l(\alpha) \propto T(\alpha)$ . Then we solve  $\dot{T}(\alpha) = 0$ .

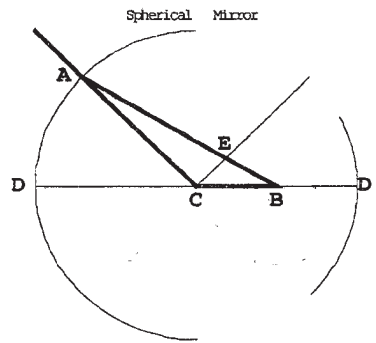


Figure 6

The light propagation time at the trajectory CDB has the expression  $T(\alpha) = CA + AE + EB$ . Here  $CA = R$  and  $CB$  are known, so  $T(\alpha) = 2R + CB \cos \alpha$ ,  $\dot{T}(\alpha) = -CB \sin \alpha$ . Therefore,  $\dot{T}(\alpha) = 0$  if and only if  $\alpha = 0$ ,  $\alpha = \pi$  in terms of this practical application we get rid of its periodic multiples. The calculation of  $\ddot{T}(\alpha)$  and its immediate evaluation at the critic points show that  $\alpha = 0$  is a feasible ray path with greatest light time propagation function ( $\ddot{T}(\alpha = 0) = -CB$ ). On the contrary,  $\alpha = \pi$  is the other feasible ray path but this linear trajectory minimizes ( $\ddot{T}(\alpha = \pi) = CB$ ) the ray path propagation time between C and B endpoints placed at the virtual normal of the spherical mirror. The monoparametric ( $\alpha$ ) propagation time function between the only two feasible ray paths consistent with Fermat's Principle one  $(C \rightarrow D \rightarrow C \rightarrow B)_{\alpha=0}$  is the maximum, and the other  $(C \rightarrow B \rightarrow D \rightarrow B)_{\alpha=\pi}$  is the minimum. Therefore, rays obeying the law of reflection  $\theta_i = \theta_r$  occasionally maximize as well as minimize travel time. There are even valid ray paths which neither maximize nor minimize the travel time function. For instance, rays beginning at the center of a spherical mirror and reflecting from it anywhere on the surface and returning to the center all have the same path length  $T(\alpha) = 2R$  and travel time. These and another exceptions to the Principle of Least Time involve reflection in special circumstances.

Farther along with our aim to contribute by a close theoretical example for testing any approximated technique we analyze the consistence of the *Reflection's Law* as a *Least Time Principle* at the for us sired quasi-spherical mirror device in terms of bringing about an application. We conceive a quasi-spherical mirror by fitting  $n$  flat mirrors with its mid-

the point sited on each  $\sqrt[n]{1}$  points and whose respective principal normals pointed toward the hub of the unitary circle. We use the eponym Fermatian associated to every light ray path that undergoes the law of reflection, it means, the angle the incident ray makes with each flat mirror's normal,  $\theta_i$ , equals the angle the reflected ray makes with its normal,  $\theta_r$ , i.e.  $\theta_i = \theta_r$ .

Our computational results make evident that if the number of flat mirrors joined is odd and focusing on hamiltonian cyclic paths certain Fermatian's cyclic rays minimize the total time light propagation multiparameter function as well others Fermatian's cyclic rays maximize the total time propagation light function. Cyclic Fermatian's minimum trajectories -module plane rotations and translations- have the regular odd polygon perimeter shape, and cyclic Fermatian's ray -module plane rotations and translations- have the odd stargon of maximum density shaped cyclic trajectories.

In contrast, whatever even-quasi-spherical mirror considered the minima are worked out by Fermatian's rays nevertheless the maxima of the time propagation light function never will be attainable to any Fermatian's ray. Precisely, the cyclic even-star regular polygon maximum density shaped paths do not reach out the maximum.

Concisely each even-stargon shaped paths and each odd-stargon shaped paths with density  $\delta \leq \lfloor \frac{n}{2} \rfloor$  all are unable to optimize the propagation time function even though they are Fermatian's rays, i.e., they are truly rays.

We show that in a quasi-spherical mirror there are feasible ray lights that propagate not always within the trajectories of least time -brachistochores-, some feasible ray propagates on cyclic trajectories spending the longest time, and what is more surprisingly of all is the existence of feasible ray light paths which neither maximize nor minimize the travel time propagation ray light function.

## 7 Conclusions

This presentation is an offspring of a series of related works in what we have participated from a first-borned idea posed formerly at the communication titled *Folding pathways as brachistochores* published in the Proceedings of IV Congreso Dr. A. R. Monteiro [15] and the paper *The RNA folding problem: a variational problem within an adiabatic approximation* submitted by Biophysical Chemistry, Elsevier Editor [16]. Both works have sustenance under the spirit of Pierre de Fermat's Principle. Who, focusing on many of the important facts of ray optics well known in his lifetime, quoted in "*Analysis ad Refractions*": *Nature operates by the simplest and most expeditious ways and means*. We struggle on for further goals [17], all of them maintain, like the present contribution does, the following ineffaceable footprints:

- 1) The scope is teleological, i.e., by postulating a *final cause*.
- 2) The exhaustive exploration of the configurational space is a ludicrous aim.
- 3) The overcome of the paradigm normally requires the design of the approximation techniques.
- 4) The theoretical study of cases of these benchmark problems when it brings about the exact solutions will be utilized in order to test the responses of the approximated proposal.

Under the previous framework we solve a specific *Euclidean Cyclic Hamiltonian Problem on the  $\sqrt[3]{1}$  Points* mainly by geometric consideration and related our results with an application of the renowned Fermat's light ray postulate. We show that in a quasi-spherical mirror there are feasible ray lights that propagate not always within the trajectories of least time -brachistochones-, some feasible ray propagates on cyclic trajectories spending the longest time, in other words *Nature sometimes is extravagant as well as economical* and what is more surprisingly of all is the existence of feasible ray light paths which neither maximize nor minimize the travel time propagation ray light function.

## References

- [1] **Gilles BRASSARD & Paul BRATLEY.** Fundamentals of Algorithmics. *Prentice Hall, Inc. 1996.*
- [2] **J. J. HOPFIELD & T. W. TANK.** 'Neural 'computation of decisions in optimization problems. *Biological Cybernetics, Vol. 52, pp. 141-152.*
- [3] **B. I. NIEL.** On the necessity of implementing an Artificial Neural Network for Solving A Specific Traveling Salesman Problem. *5<sup>th</sup> Congress SIGEF, Lausanne, November 1998.*
- [4] **Harold V. HENDERSON & S. R. SEARLE.** The Vec-Permutation Matrix, The Vec Operator and Kronecker Products: A Review. *Linear and Multilinear Algebra, 1981, Vol. 9, pp. 271-288.*
- [5] **Gene H. GOLUB & Charles F. VAN LOAN.** Matrix Computations. *Johns Hopkins, Third Edition, 1996.*
- [6] **Phillip A. REGALIA & Sanjit K. MITRA.** Kronecker Products, Unitary Matrices and Signal Processing Applications. *Society for Industrial and Applied Mathematics, 1989, Vol. 31, No. 4, pp. 586-613.*
- [7] **A. H. GEE, V. B. AIYER, & R. W. PRAGER.** An Analytical Framework for Optimizing Neural Networks. *Neural Networks, Vol. 6, pp. 79-97, 1993*
- [8] **Ronald E. MILLER.** Optimization Foundations and Applications. *John Wiley & Sons, Inc., 2000.*
- [9] **Simon HAYKIN.** Neural Networks. A comprehensive foundation. *Prentice Hall, Second Edition, 1999.*
- [10] **Kishan MEHROTRA, Chilukuri K. MOHAN, & Sanjay RANKA.** Elements of Artificial Neural Networks. *Massachusetts Institute Technology, Press, 1997.*
- [11] **Richard GOLDEN .** Mathematical Methods for Neural Network Analysis and Design. *Massachusetts Institute Technology, Press, 1997.*
- [12] **H. S. M. COXETER.** Introduction to Geometry. *John Wiley & Sons, Inc., 1961.*
- [13] **Don S. LEMONS.** Perfect Form. Variational Principles, Methods, and Applications in Elementary Physics. *Princeton University Press, Inc. 1997.*



- [14] **Fred BUCKLY & Frank HARARY.** Distance in Graphs. *Addison-Wesley Publishing Company, 1990.*
- [15] **Ariel FERNANDEZ & B. I. NIEL.** Folding pathways as brachistochrones. *Proceeding Volume of IV Congreso Dr. Antonio A. R. Monteiro.* (pg. 187-198) 15/03/97
- [16] **A. FERNANDEZ, B. I. NIEL & T. BURASTERO.** The RNA folding problem: a variational problem within an adiabatic approximation. *Biophysical Chemistry* 74(1998) 89-98.
- [17] **B. I. NIEL.** “ $\alpha$  - Levels in attraction basins: Neural Classifier ”. *International Conference in Modeling, Simulation and Neural Networks. Univ. de los Andes. Mérida, October 23<sup>th</sup> 2000. Venezuela.*